1-1-1998

Optical determination of shallow carrier profiles using Fourier transform infrared ellipsometry

Thomas E. Tiwald
University of Nebraska - Lincoln

John A. Woollam
University of Nebraska-Lincoln, jwoollam1@unl.edu

John A. Woollam
University of Nebraska - Lincoln

Optical determination of shallow carrier profiles using Fourier transform infrared ellipsometry

Thomas E. Tiwald,[a] Daniel W. Thompson, and John A. Woollam
Center for Microelectronic and Optical Materials Research, and Department of Electrical Engineering, University of Nebraska, Lincoln, Nebraska 68588-0511

(Received 6 April 1997; accepted 26 September 1997)

Dopant profiles were determined by *ex situ* Fourier transform infrared variable-angle spectroscopic ellipsometry. The technique exploits carrier absorption in the mid-infrared spectral range and combines the sensitivity of ellipsometry with a simple Drude free carrier absorption model to determine the carrier profile. The noncontact, nondestructive nature of the measurement suggests both *ex situ* and *in situ* monitoring and control applications. In this study, the carrier profiles were modeled as graded multilayers that can be constrained to a given functional form (Gaussian, erfc, etc.) when desired. Boron and arsenic implanted silicon wafers that were rapid thermal anneal and furnace annealed were measured and compared to spreading resistance probe data. © *1998 American Vacuum Society.* [S0734-211X(98)02201-X]

I. INTRODUCTION

The mid- and far-infrared spectra of doped semiconductors are often dominated by free carrier optical absorption, and these effects have been widely studied (e.g., see Refs. 1 and 2). Because of the direct dependence of the absorption on carrier density, bulk carrier densities have been determined using transmission and reflection infrared spectroscopy.[1] If the surface layers have different carrier densities than the substrate, optical interference effects allow one to measure the thickness of those layers. This has been commonly used to measure thickness of homoepitaxial layers on silicon.[3] Wagner and Schaefer,[4] Engstrom,[5] and Borghesi *et al.*[6] employed a more sophisticated graded multilayer optical model to describe the optical interference effects of ion implanted doping profiles.

In this study, we have employed a similar graded multilayer model to determine carrier concentration profiles from *ex situ* infrared spectroscopic ellipsometry (IR-SE) data. Reflection-mode ellipsometry has several advantages over simple reflectivity measurements. First, ellipsometry simultaneously determines both the real and imaginary components of the sample optical response without resorting to transmission measurements or the spectral extrapolations required for Kramers–Kronig analysis. Second, the relative phase information contained in ellipsometric spectra is highly sensitive to thin layers and microstructural effects. Finally, ellipsometry is a ratiometric measurement; therefore variations in source intensity and ambient gas absorptions are automatically factored out without resorting to dual-beam configurations or background subtraction. The ambient was not purged during these measurements.

II. EXPERIMENT

The samples consisted of ⟨100⟩ silicon that had been implanted with 20 keV B or 80 keV As at doses of 10^{15} cm^{-2} and then annealed either in a furnace or rapid thermal annealing (RTA) system. The spreading resistance probe (SRP) data were acquired by Solid State Measurements, Inc. of Pittsburgh, PA.

The infrared variable angle spectroscopic ellipsometer setup is shown in Fig. 1. It consists of a commercially available Fourier transform infrared spectrometer source (BOMEM MB102), a rotating polarizer, a high precision $\theta - 2\theta$ stage, and a rotating compensator, all under computer control. A paraboloidal mirror with a 50 cm focal length reduces the beam to a 8 mm spot at the sample, with a 3° angular spread. Intensity spectra are obtained at a number of compensator and polarizer azimuth angles. From this information, the ellipsometric ψ and Δ spectra are determined.[7] For this study, the spectral range was 700–5500 cm^{-1} (1.8–14.2 μm, 0.089–0.681 eV) at a resolution of 8 cm^{-1}.

Ellipsometry measures the change in the polarization state of light as it reflects from a sample surface. That change is expressed as the ratio of the complex Fresnel reflection coefficients r_p and r_s (for light polarized parallel and perpendicular to the plane of incidence, respectively).[8] That ratio is

$$\rho = \frac{r_p}{r_s} = \tan(\Psi) e^{i\Delta}. \tag{1}$$

Specifically, tan(Ψ) [tan(Psi)] is the ratio of the magnitudes of r_p and r_s, and Δ (delta) is the phase difference between the coefficients. Values for ψ and Δ at each wavelength comprise the ellipsometric spectra.

III. GRADED MULTILAYER DRUDE MODEL

The samples were modeled with up to 30 layers. (In many cases, 10 layers fit the data fairly well. However, adding layers generally improved the fit, with the point of diminishing returns occurring at something less than 30 layers.) The optical properties of each layer were defined by the classical Drude equation

$$\epsilon_j = \epsilon_\infty - \frac{4\pi N_j e^2}{m^*} \frac{\hbar^2}{E^2 + (i\hbar E)/\tau}, \tag{2}$$

[a]Electronic mail: ttiwald@unlgradi.unl.edu

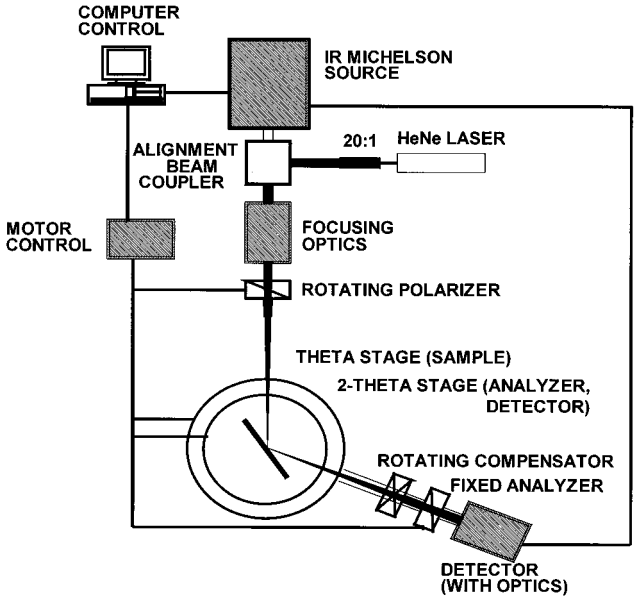

FIG. 1. Schematic of the infrared variable angle spectroscopic ellipsometer used in this study.

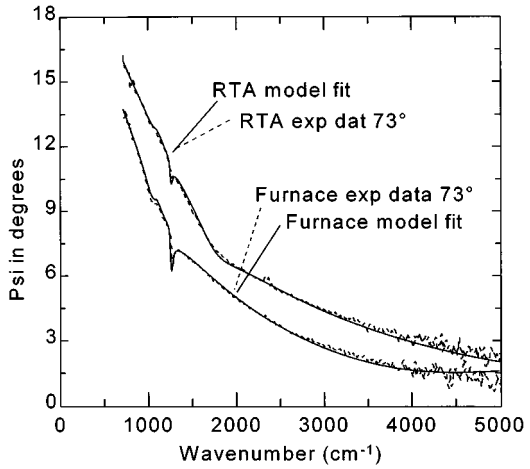

FIG. 3. Ellipsometric psi (Ψ) spectra for 73° angle of incidence (measured and optimized model fit) for 10^{15} As/cm^{-2} samples (RTA and furnace annealed).

where ϵ_j is the complex dielectric constant of the jth layer, ϵ_∞ is the high frequency dielectric response of the tightly bound core electrons, N_j is the jth layer carrier concentration, e is the electronic charge, m is the ratio of the optical carrier effective mass to the electron rest mass, E is the energy of the incident photons, and τ is the mean scattering time. The quantities ϵ_∞, m^*, and τ were the same for all layers. However, the quantity N_j was allowed to vary as a function of the following Gaussian distribution:

$$N_j = N_{\max} \exp\left[-\frac{1}{2} \left(\frac{(j/n)d - R_p}{\Delta R_p} \right)^2 \right]. \quad (3)$$

In Eq. (3), d is the total thickness of the graded multilayer, and n is the total number of layers. R_p is the range and ΔR_p is the standard deviation. The result is a Gaussian dielectric function profile for each wavelength in the spectral range of interest. For example, Fig. 2 shows the imaginary part of a Gaussian dielectric profile for a 0.0992 eV photon energy. Other functions can be substituted for the right hand side of Eq. (3) [e.g., the erfc(x)]. The N_j for each layer can also be allowed to vary randomly.

To summarize the optical model, it consisted of 30 layers, with the optical properties of each layer defined by the classical Drude model. The values ϵ_∞ and τ were the same for all layers, but in this study N_j varied as a Gaussian function of depth. The optical effective mass cannot be independently determined because it is completely correlated with N_j in the ratio N_j/m^* by Eq. (1). Therefore m^* was fixed at appropriate values taken from the literature.[9,10]

IV. NUMERICAL DATA ANALYSIS

During data analysis $N_{\max}$, R_p, ΔR_p, ϵ_∞, and τ were adjusted to minimize the mean squared error (MSE) between the calculated ellipsometric response of the model and the measured response of the sample. The numerical analysis

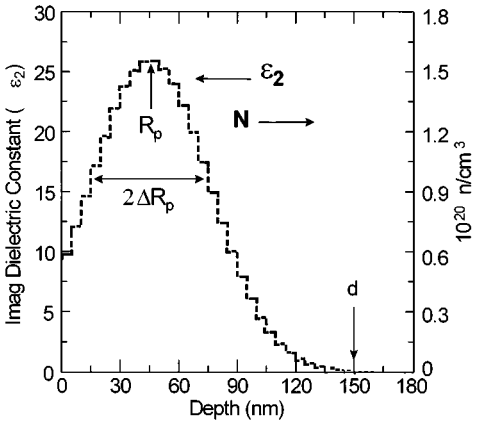

FIG. 2. Imaginary part of the dielectric function for a Gaussian multilayer optical model at a photon energy of 0.0992 eV (800 cm^{-1}).

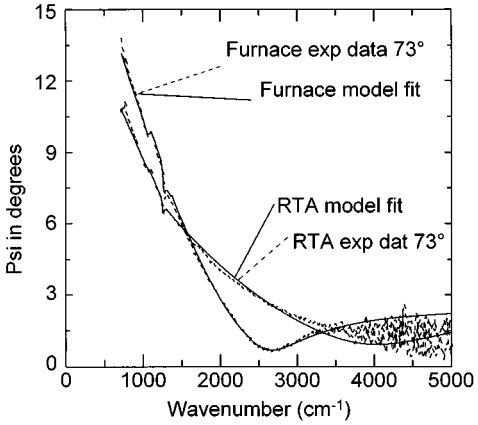

FIG. 4. Ellipsometric psi (Ψ) spectra 73° angle of incidence (measured and optimized model fit) for 10^{15} B/cm^{-2} samples (RTA and furnace annealed).

TABLE I. Optimized model parameters from ellipsometric data. The effective mass, m^*, was estimated using values from van Driel (Ref. 10).

Implant species	Dose (cm^{-2})	Anneal	N_{max} (cm^{-3})	R_p (nm)	ΔR_p (nm)	τ (10^{-15} s)	ϵ_∞	m^*	Measured dose (cm^{-2})	t oxide (nm)
As 80 keV	10^{15}	RTA	1.3×10^{20}	44	32	11	12.5	0.3	9.1×10^{14}	3.4
		furnace	4.8×10^{19}	52	74	12	12.5	0.28	6.8×10^{14}	6.6
B 20 keV	10^{15}	RTA	9.3×10^{19}	92	38	7.5	12.8	0.4	8.7×10^{14}	1.7
		furnace	4.0×10^{19}	115	190	6.7	12.6	0.38	1.5×10^{15}	4.6

was initiated by inserting starting values for the parameters into Eqs. (2) and (3), from which the spectrally dependent dielectric constant for each of layer was calculated. The ellipsometric response ρ [Eq. (1)] of the entire model was then determined using the scattering matrix method.[8] This procedure was repeated using the nonlinear Levenberg–Marquardt algorithm[11] to adjust the fitting parameters N_{max}, R_p, ΔR_p, ϵ_∞, and τ until a minimum MSE between the calculated and measured ellipsometric values were achieved.

Figure 3 shows the measured ellipsometric spectra (for brevity, only Psi is shown) for 10^{15} cm^{-2} 80 keV As implant samples, along with the spectra calculated from the best fit (optimized) Gaussian multilayer model. Similarly, Fig. 4 shows the same Psi spectra for the 10^{15} 20 keV B cm^{-2} samples. Clearly, the generated data from the optimized model fits the various features of the measured spectra, particularly for the arsenic samples. The sharp feature at 1250 cm^{-1} is an effect of the native oxide, which was included in the model as a uniform layer using the bulk SiO_2 glass optical constants found in Palik,[12] and fitting for thickness. The model parameters for the four samples are listed in Table I.

Figures 5 and 6 compare the Gaussian carrier profiles determined by IR-SE to SRP data from the same samples. As Fig. 5 shows, IR-SE and SRP curves match quite well for the arsenic samples, but differ for the boron samples. A closer examination of the SRP data shows that the boron profile is not Gaussian, so it is not surprising that IR-SE Gaussian model does not match the SRP profile.

For the boron samples, the mean scattering time τ of 6.7×10^{-15} and 7.5×10^{-15} s (see Table I) agrees with the values of Borghesi *et al.*[6] for peak concentrations in the 10^{19} cm^{-3} range. Similarly, the arsenic samples had τ values around 11×10^{-15} s, which agrees with Miyoa *et al.*[9] for peak concentrations of 10^{20} cm^{-3} among the four samples.

For all the samples, the parameter ϵ_∞ ranges from 12.5 to 12.8. This value is consistently larger then 11.7, as one might expect for silicon in the mid-IR.[6,13] Given the infrared-transparent nature of silicon, it is reasonable to assume that some of the back-surface reflections would affect the data, particularly in the near-IR wavelength region where ϵ_∞ is most sensitive to ellipsometric data. This effect was not taken into account in the model, and might account for the discrepancy between these results and the literature.

V. CONCLUSIONS

The data clearly show that IR-SE is sensitive to the anneal conditions (RTA vs furnace) for ion-implanted silicon samples. Also, the arsenic data were reasonably represented by Gaussian carrier profiles that match the SRP results. For boron implants, the non-Gaussian SRP profiles do not match the IR-SE Gaussian model. These results indicate a need for the development of graded-multilayer models that are not constrained exclusively to a Gaussian profile or other simple mathematical functions.

This study is a first step in exploring this noncontact, nondestructive technique. Further work will include addi-

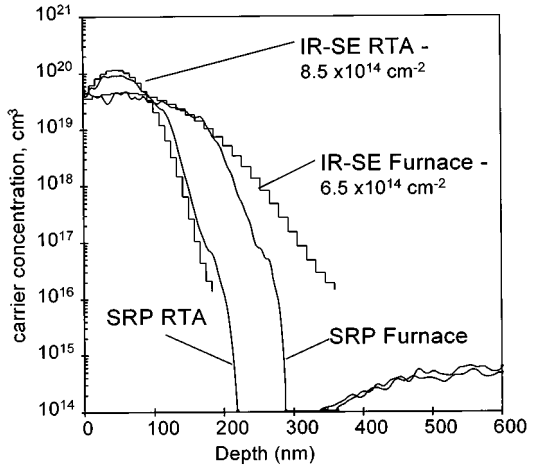

FIG. 5. IR-SE and SRP carrier distributions for the 10^{15} As/cm^{-2} and integrated carrier doses for RTA and furnace anneal samples.

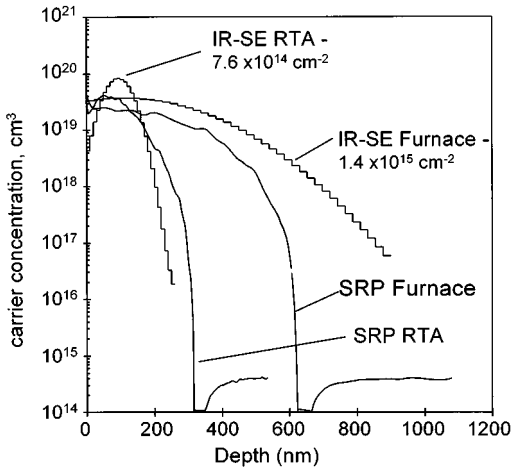

FIG. 6. IR-SE and SRP carrier distributions for the 10^{15} B/cm^{-2} and integrated carrier doses for RTA and furnace anneal samples.

tional SRP and SIMS comparisons, particularly ultrashallow junction profiles. Refinements in the carrier distribution model are also needed. Besides the expansion beyond strictly Gaussian distributions mentioned above, a refined model might accommodate damaged layers by including layer-to-layer variations in the mean scattering time τ and the high frequency dielectric response ϵ_∞. Finally, extending the wavelength range to longer wavelengths would increase the sensitivity to lower carrier concentrations.

ACKNOWLEDGMENTS

The authors would like to thank Wayne Paulson and Robert Hance of Motorola Semiconductor Products Sector for providing samples.

[1]C. R. Pidgeon, in *Handbook on Semiconductors*, Vol. 2, edited by T. S. Moss and Minko Balkanski (North Holland, Amsterdam, 1980), pp. 227–230.
[2]B. Jensen, *Handbook of Optical Constants of Solids*, edited by E. D. Palik (Academic, Boston, 1985), p. 169.
[3]K. Krishnan and P. J. Stout, *Practical Fourier Transform Infrared Spectroscopy*, edited by J. R. Ferraro and K. Krishnan (Academic, Orlando, 1990), p. 285.
[4]H. H. Wagner and R. R. Schaefer, J. Appl. Phys. **50**, 2697 (1979).
[5]H. Engstrom, J. Appl. Phys. **51**, 5245 (1980).
[6]A. Borghesi, C. Chen-Jia, G. Guizzetti, L. Nosenzo, A. Stella, S. U. Campisano, and E. Rimini, J. Appl. Phys. **58**, 2773 (1985).
[7]P. S. Hauge, Surf. Sci. **56**, 148 (1976).
[8]R. M. A. Azzam and N. M. Bashara, *Ellipsometry and Polarized Light* (North–Holland, New York, 1977), Chap. 4, pp. 273, 332.
[9]M. Miyao, T. Motooka, N. Natsuaki, and T. Tokuyama, Solid State Commun. **37**, 605 (1981).
[10]H. M. van Driel, Appl. Phys. Lett. **44**, 617 (1984).
[11]W. H. Press, B. P. Flannery, S. A. Teukolsky, and W. T. Vetterling, *Numerical Recipes: The Art of Scientific Computing* (Cambridge University Press, Cambridge, MA, 1988), Chap. 14.
[12]H. R. Philipp, *Handbook of Optical Constants in Solids*, edited by E. D. Palik (Academic, Boston, 1985), p. 749.
[13]W. R. Runyan, *Silicon Semiconductor Technology* (McGraw–Hill, New York, 1965), p. 199.